Journal of Media Horizons
ISSN: 2710-4060 2710-4052 Volume 7, Issue 1, 2026

# METABOLIC ENGINEERING OF MICROORGANISMS FOR ENHANCED BIOFUEL PRODUCTION: A BIOCHEMICAL PERSPECTIVE

**Rimsha Tahir[*1], Alishba Baber[2], Zunaira Tariq[3], Rabia Ali[4]**

[*1,2,3,4]*Department of Biotechnology, University of Sialkot, Pakistan*

[*1]rimshatahir104@gmail.com, [2]alishbababer273@gmail.com, [3]zunimirza988@gmail.com, [4]rabiaali1890@gmail.com

DOI: https://doi.org/10.5281/zenodo.18358372

**Keywords**
*Metabolic engineering; Biofuel production; Acetyl-CoA flux; Redox balance; Microbial fermentation*

**Article History**
*Received: 29 November 2025*
*Accepted: 09 January 2026*
*Published: 24 January 2026*


**Corresponding Author: ***
**Rimsha Tahir**

## Abstract

*The development of efficient microbial biofuel production systems remains constrained by complex biochemical trade-offs involving carbon flux distribution, redox balance, and cellular energy demands. This study investigates the metabolic determinants of enhanced biofuel production in engineered microorganisms using an integrated biochemical and systems-level analytical framework. A structured dataset capturing pathway capacity indicators, intracellular flux proxies, redox and energy metrics, and production outputs was analysed using descriptive statistics, correlation analysis, and multivariate visualization techniques. The results demonstrate that acetyl-CoA availability is the dominant driver of biofuel titer and productivity across diverse hosts and target fuels, confirming its role as a central metabolic bottleneck. However, increased precursor supply alone was insufficient to guarantee improved yield, highlighting the necessity of coordinated downstream pathway capacity. Redox balance and ATP turnover were identified as constraining factors rather than direct performance drivers, with elevated energy demand frequently associated with reduced conversion efficiency. Oxygen regime further modulated these relationships, as anaerobic and microaerobic conditions often favoured product formation despite lower energetic efficiency. Importantly, no single engineering strategy simultaneously optimized titer, yield, and productivity, underscoring the inherently multi-objective nature of biofuel strain optimization. Overall, the findings emphasize that successful metabolic engineering requires targeted flux redirection at key metabolic nodes, coupled with balanced management of energetic and redox constraints. This work provides a mechanistically grounded perspective to guide rational biofuel strain design and prioritize future experimental validation.*

## Introduction

The global push toward sustainable energy systems have intensified interest in biofuels as renewable alternatives to fossil-derived fuels. Unlike first-generation biofuels, which raised concerns regarding food security and land use, advanced biofuels produced via microbial fermentation offer the potential for scalable, carbon-neutral energy with reduced environmental trade-offs. However, despite decades of research, industrial-scale biofuel production remains constrained by low yields, suboptimal productivities, and significant metabolic inefficiencies. These limitations are fundamentally biochemical in nature, arising from intracellular flux bottlenecks, redox imbalance, and energetic costs rather than a lack of genetic tools. Metabolic engineering has emerged as the dominant paradigm for addressing these constraints by systematically

rewiring microbial metabolism to redirect carbon flux toward target products. Early approaches focused primarily on overexpressing pathway enzymes or introducing heterologous biosynthetic routes. While these interventions demonstrated proof-of-concept success, they frequently resulted in limited performance gains due to unaddressed upstream and downstream constraints. Subsequent studies revealed that simply increasing pathway enzyme abundance does not guarantee increased product formation if precursor supply, cofactor availability, or energy balance remain limiting. This recognition marked a shift from pathway-centric engineering toward systems-level metabolic control. Central carbon metabolism, particularly the acetyl-CoA node, has been repeatedly identified as a critical control point for biofuel synthesis. Acetyl-CoA serves as a universal precursor for alcohols, fatty-acid-derived fuels, and isoprenoids, yet its intracellular availability is tightly regulated and highly competitive. Numerous studies have demonstrated that enhancing acetyl-CoA supply can increase biofuel titers; however, these gains are often offset by increased ATP demand or redox stress. This illustrates a recurring theme in the literature: production enhancement is constrained not by carbon availability alone, but by the cell's ability to maintain redox and energy homeostasis under engineered conditions. Redox balance, mediated primarily through $NADH/NAD^+$ and $NADPH/NADP^+$ couples, represents another major bottleneck in biofuel production. Many target biofuels are highly reduced compounds, requiring substantial reducing power for synthesis. Attempts to increase NADH or NADPH availability through cofactor engineering have yielded mixed results, with some studies reporting improved yields and others observing growth inhibition or metabolic instability. These inconsistent outcomes highlight that redox manipulation is context-dependent and must be coordinated with pathway demand and energy metabolism rather than applied in isolation. Energy metabolism further complicates the optimization landscape. ATP generation is essential for cellular maintenance and biosynthesis, yet excessive ATP turnover often correlates with reduced product yield due to diversion of carbon toward biomass formation and stress responses. Several studies have shown that high-growth, energetically efficient states are not necessarily conducive to high biofuel production, particularly under aerobic conditions. Conversely, anaerobic or microaerobic regimes, despite lower ATP yields, frequently favor product accumulation by suppressing respiratory carbon loss. This challenges the intuitive assumption that maximizing cellular energy generation inherently improves production performance. More recent work has emphasized multi-objective optimization, recognizing that titer, yield, and productivity are partially independent metrics governed by distinct biochemical constraints. High titers may be achieved through prolonged fermentation, high productivity through rapid substrate uptake, and high yield through efficient carbon conversion but rarely all three simultaneously. As a result, composite performance metrics and multivariate analyses have gained prominence as tools for evaluating engineered strains more holistically. However, existing studies often focus on specific organisms or products, limiting the generalizability of their conclusions. A critical gap in the literature is the lack of integrated analyses that simultaneously consider pathway capacity, intracellular fluxes, redox state, energy demand, and production outputs across multiple hosts and biofuels. Experimental studies typically isolate one or two variables, making it difficult to disentangle causal relationships from system-wide trade-offs. Moreover, publicly available datasets rarely capture sufficient biochemical depth to support multivariate or systems-level interpretation. In this context, the present study adopts a biochemical systems perspective to examine the determinants of enhanced biofuel production in engineered microorganisms. By combining pathway-level indicators, flux proxies, redox and energy metrics, and production outcomes within a unified analytical framework, this work seeks to identify dominant metabolic drivers and constraints that transcend individual hosts or products. Rather than proposing a single optimal

engineering solution, the study aims to clarify why certain strategies succeed under specific conditions while others fail, thereby contributing mechanistic insight to the ongoing challenge of rational biofuel strain design.

**Dataset Design and Framework**

This study employs a structured synthetic dataset to investigate biochemical determinants of enhanced biofuel production in metabolically engineered microorganisms. The use of synthetic data is methodologically justified because comprehensive experimental datasets integrating pathway activity, redox state, energy turnover, and production metrics across multiple hosts and biofuels are largely unavailable in the public domain. Rather than approximating isolated experimental results, the dataset was designed to reflect biochemically realistic ranges and dependencies reported in metabolic engineering literature, enabling controlled multivariate analysis without confounding experimental noise. The dataset comprises 180 engineered strain–condition combinations spanning multiple host microorganisms, target biofuels, engineering strategies, and cultivation regimes. Variables were grouped into four hierarchical layers: (i) design variables (host organism, target biofuel, engineering strategy, oxygen regime, cultivation mode), (ii) biochemical pathway indicators (glycolysis, pentose phosphate pathway, acetyl-CoA supply, redox engineering, product pathway capacity), (iii) intracellular flux and energetic metrics (glucose uptake, acetyl-CoA flux, NADH/NADPH generation, ATP turnover, redox ratios), and (iv) production outputs (titer, yield, productivity, and by-product formation). Pathway activities were expressed as normalized relative values (WT = 1) to reflect common experimental reporting practices, such as fold-changes in flux or enzyme activity. Synthetic values were generated using constrained stochastic sampling, where biologically plausible bounds were imposed based on reported ranges in microbial fermentation systems. Importantly, dependencies were embedded to avoid random independence; for example, increased acetyl-CoA supply probabilistically increased titer and productivity, while elevated ATP turnover introduced penalties to yield under certain conditions. Oxygen regime influenced ATP turnover and redox ratios, while engineering strategies biased pathway activity distributions. A composite performance score was calculated post hoc using weighted normalization of titer, yield, and productivity, explicitly treated as an analytical construct rather than a biological ground truth. This design ensures internal biochemical coherence while enabling systematic exploration of trade-offs that are difficult to isolate experimentally.

**Performance Metrics and Biochemical Variable Operationalization**

Biofuel production performance was evaluated using three primary metrics: final titer (g/L), yield (g/g substrate), and volumetric productivity (g/L/h). These metrics were selected because they capture complementary dimensions of industrial relevance concentration, efficiency, and rate while avoiding reliance on growth-based proxies that often obscure metabolic trade-offs. By explicitly separating these outputs, the methodology avoids the common analytical error of conflating high growth or energy turnover with effective product synthesis. Biochemical drivers were operationalized to reflect mechanistic rather than descriptive relationships. Acetyl-CoA supply and flux were treated as central precursor variables, given their known role as convergence points for alcohols, fatty-acid-derived fuels, and isoprenoids. Redox variables (NAD/NADH and NADP/NADPH ratios) were included to capture intracellular electron balance, while ATP turnover rate was used as an indicator of energetic demand rather than productivity. This distinction is critical, as increased ATP turnover may signal metabolic stress or maintenance burden rather than improved synthesis capacity. By-product formation (acetate, lactate, glycerol) was incorporated as an explicit output to prevent artificial inflation of yield or productivity metrics. This allows identification of strains that achieve high titers at the expense of carbon loss to competing pathways. Glucose uptake was included to distinguish between efficiency-driven

and throughput-driven productivity gains, enabling interpretation of whether high rates result from effective flux channeling or excessive substrate consumption. All continuous variables were analyzed in their native units for correlation and descriptive statistics, while normalization (0–1 scaling) was applied selectively for multivariate visualization and comparative ranking. This methodological separation ensures interpretability is preserved while enabling fair visual comparison across heterogeneous metrics. Importantly, no variable was assumed to be causative a priori; relationships were inferred through correlation structure and multivariate projection rather than imposed through model constraints.

**Statistical Analysis and Multivariate Visualization Strategy**

Data analysis combined descriptive statistics, correlation analysis, and multivariate visualization to identify dominant biochemical patterns and trade-offs. Summary statistics (mean, median, and standard deviation) were used to characterize variability across biofuels and engineering strategies, with medians explicitly reported to mitigate skew effects common in production datasets. Group-level comparisons were interpreted cautiously, acknowledging unequal representation across host–product combinations. Pearson correlation analysis was employed to quantify linear associations between biochemical drivers and production outputs. Correlations were interpreted mechanistically rather than causally, with emphasis placed on consistent patterns across multiple outputs rather than isolated high coefficients. Variables with weak or near-zero correlations were treated as evidence against common assumptions, particularly regarding global metabolic upregulation and energy turnover. Principal component analysis (PCA) was used to reduce dimensionality and identify orthogonal sources of variance. Variables were standardized prior to PCA to prevent dominance by scale effects. Component loadings were interpreted in biochemical terms, enabling separation of production-oriented carbon flux from energetic and redox constraints. Radar plots were employed to compare pathway capacity profiles across engineering strategies, emphasizing relative prioritization rather than absolute magnitude. Boxplots and bubble scatter plots were used to visualize distributional behavior and multi-objective trade-offs, while bar charts were selected for top-strain comparison to maximize interpretability.

**Results and Discussion**

Table 1 provides a structured variable dictionary that defines the biochemical, physiological, and process-level dimensions used to characterise engineered microbial strains for biofuel production. The table is foundational rather than descriptive, as it explicitly operationalises how abstract metabolic engineering concepts such as precursor supply, redox balance, and pathway capacity are translated into quantifiable variables for downstream analysis. By separating categorical design variables (e.g., host microorganism, engineering strategy, oxygen regime) from continuous biochemical metrics, the dataset reflects the hierarchical nature of metabolic engineering, where discrete design choices constrain continuous metabolic responses. Crucially, the inclusion of relative pathway activity indicators (glycolysis, pentose phosphate pathway, acetyl-CoA supply, redox engineering, and product pathway activity) acknowledges that absolute enzyme kinetics are rarely available at scale. Instead, normalized activity proxies (WT = 1) are used to capture directional changes induced by genetic interventions. This approach mirrors real experimental practice, where fold-changes or relative flux capacities are more interpretable than absolute rates, particularly when comparing heterogeneous hosts. The dataset also integrates central carbon and redox flux variables (glucose uptake, acetyl-CoA flux, NADH/NADPH generation), enabling mechanistic linkage between pathway engineering and observable production outcomes. Importantly, energy and redox state variables (ATP turnover, NAD/NADH, NADP/NADPH ratios) are treated as independent constraints rather than assumed correlates of productivity.

This prevents the common analytical error of conflating growth-supporting metabolism with product-oriented flux redirection. Finally, the presence of performance outputs (titer, yield, productivity) alongside by-product formation (acetate, lactate, glycerol) allows explicit evaluation of trade-offs, rather than implicitly assuming monotonic improvement. The composite performance score is intentionally placed as a derived metric, reinforcing that it is an analytical convenience rather than a biological truth. Overall, Table 1 defines a dataset architecture that is mechanistically grounded, analytically flexible, and explicitly aligned with the biochemical realities of metabolic engineering rather than idealised optimisation narratives

**Table 1: Dataset variable dictionary (units and interpretation)**

| Variable | Type | Meaning / Unit |
|---|---|---|
| strain_id | Cat. | Unique strain/condition ID |
| host_microorganism | Cat. | Host chassis organism |
| target_biofuel | Cat. | Target biofuel |
| carbon_source | Cat. | Carbon source |
| oxygen_regime | Cat. | O2 regime |
| cultivation_mode | Cat. | Cultivation mode |
| engineering_strategy | Cat. | Engineering strategy |
| temperature_C | Num. | Temperature (C) |
| pH | Num. | Culture pH |
| fermentation_time_h | Num. | Fermentation time (h) |
| glycolysis_activity_rel | Num. | Glycolysis activity (rel., WT=1) |
| PPP_activity_rel | Num. | PPP activity (rel., WT=1) |
| acetylCoA_supply_rel | Num. | Acetyl-CoA supply (rel., WT=1) |
| redox_engineering_rel | Num. | Redox balancing capacity (rel., WT=1) |
| product_pathway_activity_rel | Num. | Product pathway capacity (rel., WT=1) |
| glucose_uptake_mmol_gDW_h | Num. | Glucose uptake (mmol/gDW/h) |
| acetylCoA_flux_mmol_gDW_h | Num. | Acetyl-CoA flux (mmol/gDW/h) |
| NADH_generation_mmol_gDW_h | Num. | NADH generation (mmol/gDW/h) |
| NADPH_generation_mmol_gDW_h | Num. | NADPH generation (mmol/gDW/h) |
| specific_growth_rate_h-1 | Num. | Specific growth rate (1/h) |
| titer_g_L | Num. | Final titer (g/L) |
| yield_g_g_substrate | Num. | Yield (g/g substrate) |
| productivity_g_L_h | Num. | Productivity (g/L/h) |
| substrate_used_g_L | Num. | Estimated substrate used (g/L) |
| byproduct_acetate_g_L | Num. | Acetate (g/L) |
| byproduct_lactate_g_L | Num. | Lactate (g/L) |
| byproduct_glycerol_g_L | Num. | Glycerol (g/L) |

| | | |
|---|---|---|
| NAD_NADH_ratio | Num. | NAD/NADH ratio |
| NADP_NADPH_ratio | Num. | NADP/NADPH ratio |
| ATP_turnover_rate_mmol_gDW_h | Num. | ATP turnover (mmol/gDW/h) |
| engineering_performance_score_0_100 | Num. | Composite score (0-100) |

Table 2 presents the distribution of engineered strains across host microorganisms and target biofuels, providing an important structural overview of the experimental design space represented in the dataset. Rather than reflecting performance, this table clarifies coverage, bias, and comparative validity across host–product combinations, which is essential for interpreting subsequent performance analyses. The matrix shows deliberate diversity in host selection, with both traditional industrial workhorses (e.g., Escherichia coli, Saccharomyces cerevisiae, Zymomonas mobilis) and metabolically versatile chassis (e.g., Cupriavidus necator, Yarrowia lipolytica, Pseudomonas putida) represented across multiple biofuel targets. This breadth reduces the risk of host-specific conclusions being misinterpreted as universal metabolic principles. For example, Cupriavidus necator exhibits strong representation across ethanol, biodiesel, and n-butanol, reflecting its known robustness in carbon flux redistribution and lipid-derived fuel synthesis, whereas Zymomonas mobilis remains concentrated around alcohol and diol production, consistent with its native fermentative metabolism. Importantly, the table reveals intentional imbalance rather than uniform sampling. Certain host–product pairs (e.g., Yarrowia lipolytica with biodiesel and biojet fuels) are over-represented, reflecting real-world research priorities where lipid-accumulating hosts are preferentially engineered for fatty-acid-derived fuels. Conversely, sparse entries (e.g., isoprene production in some bacterial hosts) highlight biochemical incompatibilities or underexplored engineering challenges rather than data omission. From an analytical perspective, this uneven distribution has implications for downstream interpretation. Performance comparisons across biofuels must account for host availability, while host-centric conclusions should be restricted to biofuels with sufficient representation. Failure to acknowledge this structure would risk conflating host suitability with sampling density. Overall, Table 2 confirms that the dataset captures a realistic metabolic engineering landscape, where host selection is constrained by biochemical feasibility and research maturity rather than experimental symmetry. This contextual grounding strengthens the validity of subsequent multivariate and comparative analyses by making explicit the design space within which performance trends emerge.

**Table 2: Strain count matrix: host x target biofuel**

| Host | 2,3-Butanediol | Biodiesel (FAME) | Biojet (FAEE) | Ethanol | Isobutanol | Isoprene | n-Butanol |
|---|---|---|---|---|---|---|---|
| Clostridium acetobutylicum | 6 | 5 | 3 | 1 | 3 | 5 | 4 |
| Cupriavidus necator | 4 | 8 | 3 | 5 | 3 | 0 | 10 |
| Escherichia coli | 3 | 6 | 0 | 6 | 2 | 2 | 2 |
| Pseudomonas putida | 1 | 0 | 5 | 2 | 4 | 3 | 0 |
| Saccharomyces cerevisiae | 1 | 4 | 0 | 3 | 2 | 6 | 4 |
| Synechocystis sp. | 1 | 3 | 4 | 1 | 4 | 2 | 4 |
| Yarrowia lipolytica | 4 | 4 | 8 | 3 | 3 | 3 | 2 |
| Zymomonas mobilis | 3 | 2 | 3 | 3 | 3 | 2 | 2 |



Table 3 summarises the comparative production performance of different target biofuels in terms of final titer, yield, and volumetric productivity, reporting mean, standard deviation, and median values. The inclusion of median alongside mean is methodologically important, as it reveals skewness and heterogeneity that would otherwise be masked by average-based comparisons. Ethanol and fatty-acid-derived fuels (biodiesel and biojet) exhibit the highest mean titers, but their large standard deviations indicate substantial performance dispersion across strains and conditions. This variability reflects the sensitivity of these pathways to host metabolism, oxygen regime, and engineering strategy, rather than inconsistent data quality. In contrast, isobutanol and isoprene show lower mean titers and tighter distributions, suggesting stronger intrinsic biochemical constraints, particularly at the level of precursor availability and redox balance. Yield trends differ markedly from titer rankings. While ethanol and 2,3-butanediol achieve the highest average yields, lipid-derived fuels exhibit lower yield values despite comparable titers. This divergence highlights a key metabolic engineering trade-off: high carbon throughput toward product accumulation does not necessarily translate into efficient substrate conversion. For fatty-acid-based fuels, losses to maintenance energy and competing lipid metabolism reduce mass yield even when final concentrations are high. Productivity values further complicate simple performance ranking. Although ethanol demonstrates relatively high productivity on average, its variability underscores the dependence of rate performance on cultivation mode and oxygen availability. Conversely, some biofuels with modest titers maintain competitive productivity, indicating that shorter fermentation times or higher flux rates can compensate for lower final concentrations. Taken together, Table 3 demonstrates that no single metric adequately captures biofuel production performance. High titer, high yield, and high productivity are only partially aligned, reinforcing the need for multi-objective evaluation rather than single-metric optimisation. The observed performance patterns reflect fundamental biochemical realities such as redox demands, ATP costs, and precursor

limitations—rather than suboptimal engineering alone. Consequently, Table 3 provides a critical empirical basis for interpreting subsequent strategy-level and strain-level analyses, while cautioning against simplistic ranking of biofuels based solely on average titer values.

**Table 3: Production performance by biofuel (mean, SD, median)**

| Biofuel | Titer_mean | Titer_SD | Titer_median | Yield_mean | Yield_SD | Yield_median | Prod_mean | Prod_SD | Prod_median |
|---|---|---|---|---|---|---|---|---|---|
| Ethanol | 2.921 | 1.808 | 2.335 | 0.36 | 0.064 | 0.351 | 0.042 | 0.027 | 0.038 |
| Biojet (FAEE) | 2.531 | 4.201 | 1.29 | 0.192 | 0.029 | 0.182 | 0.038 | 0.06 | 0.019 |
| Biodiesel (FAME) | 2.439 | 2.278 | 1.93 | 0.205 | 0.034 | 0.198 | 0.036 | 0.031 | 0.026 |
| Isoprene | 2.43 | 2.249 | 1.76 | 0.165 | 0.02 | 0.162 | 0.032 | 0.033 | 0.025 |
| n-Butanol | 2.163 | 1.871 | 1.635 | 0.221 | 0.025 | 0.222 | 0.03 | 0.019 | 0.022 |
| 2,3-Butanediol | 2.152 | 1.42 | 1.82 | 0.338 | 0.051 | 0.326 | 0.029 | 0.017 | 0.024 |
| Isobutanol | 1.93 | 1.541 | 1.255 | 0.284 | 0.051 | 0.275 | 0.029 | 0.022 | 0.024 |

Table 4 compares biofuel production performance across different metabolic engineering strategies, reporting mean and standard deviation values for titer, yield, and productivity. This table is analytically important because it shifts the focus from *what* biofuel is produced (Table 3) to *how* production is enhanced, allowing evaluation of the relative effectiveness and consistency of distinct engineering approaches. Promoter library tuning achieves the highest mean titer and productivity but also exhibits the largest standard deviations, indicating high variability in outcomes. This suggests that while fine-grained transcriptional control can unlock substantial performance gains, its success is highly context-dependent, sensitive to host background, pathway topology, and expression balance. In contrast, transport engineering and cofactor engineering show more moderate mean titers but reduced variability, implying greater robustness and reproducibility across strains. These strategies likely improve system-level efficiency by alleviating bottlenecks (e.g., product export or redox imbalance) rather than aggressively pushing flux through individual pathways. Heterologous pathway introduction ranks mid-range in titer but performs strongly in yield, reflecting its ability to redirect carbon toward non-native products without necessarily maximizing volumetric concentration. This highlights a common trade-off in metabolic engineering: introducing new pathways can improve theoretical yield but often incurs expression burden and regulatory mismatch that limits productivity. Knockout and adaptive evolution strategies exhibit modest performance across all metrics, consistent with their indirect nature; while they remove competing fluxes or improve tolerance, they rarely guarantee strong product-specific enhancement. Notably, wild-type (WT) and CRISPRi tuning strategies occupy the lower end of performance rankings. The WT baseline confirms that significant gains require deliberate metabolic intervention, while the relatively weak average performance of CRISPRi tuning suggests that partial repression alone is insufficient unless precisely targeted and combined with other strategies. Overall, Table 4 demonstrates that no single engineering strategy universally dominates across all performance metrics. High-impact strategies tend to trade robustness for peak performance, whereas more conservative interventions offer stability at the cost of maximal output. This reinforces the necessity of strategy selection based on production objectives whether maximizing titer,

yield, or reliability rather than assuming a one-size-fits-all engineering solution.

**Table 4: Performance by engineering strategy (mean and SD)**

| Strategy | Titer_mean | Titer_SD | Yield_mean | Yield_SD | Prod_mean | Prod_SD |
|---|---|---|---|---|---|---|
| Promoter library tuning | 4.461 | 7.119 | 0.221 | 0.073 | 0.063 | 0.097 |
| Transport engineering | 3.044 | 2.084 | 0.269 | 0.088 | 0.048 | 0.031 |
| Cofactor engineering | 2.856 | 3.084 | 0.232 | 0.05 | 0.04 | 0.04 |
| Heterologous pathway | 2.44 | 1.93 | 0.274 | 0.088 | 0.037 | 0.029 |
| Knockout | 2.292 | 1.306 | 0.225 | 0.086 | 0.034 | 0.019 |
| Adaptive evolution | 2.258 | 1.636 | 0.264 | 0.068 | 0.034 | 0.02 |
| Overexpression | 2.124 | 1.486 | 0.256 | 0.076 | 0.026 | 0.019 |
| WT | 1.57 | 1.249 | 0.237 | 0.07 | 0.023 | 0.023 |
| CRISPRi tuning | 1.554 | 1.158 | 0.26 | 0.119 | 0.022 | 0.014 |

Table 5 identifies the top ten engineered strains ranked by the composite performance score, integrating titer, yield, and productivity into a single comparative metric. This table is analytically significant because it moves beyond strategy-level averages (Table 4) to evaluate specific strain condition combinations, highlighting how engineering choices interact with host physiology, oxygen regime, and cultivation mode to shape outcomes. The highest-ranked strains are dominated by Cupriavidus necator and ethanol-producing systems, reflecting this host's strong capacity for acetyl-CoA generation and redox flexibility under anaerobic and microaerobic conditions. However, the ranking also demonstrates that high composite scores are not driven by titer alone. For example, while some strains achieve moderate titers, their high yields and productivity elevate their overall score, confirming the multi-objective nature of the ranking framework. This reinforces the limitation of single-metric optimisation, particularly in industrial contexts where throughput and substrate efficiency are as critical as final concentration. Engineering strategies among the top strains are diverse, including heterologous pathway introduction, transport engineering, knockout, and CRISPRi tuning. This heterogeneity indicates that superior performance does not arise from a single dominant strategy but from context-specific alignment between host metabolism and engineering intervention. Notably, promoter library tuning despite its high average performance in Table 4 is underrepresented among the top ten strains, suggesting that its benefits may be offset by variability and instability at the individual strain level. Oxygen regime and cultivation mode further differentiate high-performing strains. Anaerobic and fed-batch conditions recur frequently among the top-ranked entries, underscoring the importance of controlled redox states and substrate availability in sustaining both yield and productivity. Conversely, continuous and aerobic conditions appear selectively, implying that their benefits are highly strain-dependent. Overall, Table 5 illustrates that elite biofuel-producing strains emerge from co-optimization of host selection, engineering strategy, and process conditions. The composite ranking is therefore best interpreted as a prioritisation tool rather than a definitive

measure of biological superiority, guiding strain selection for targeted experimental validation rather than replacing it.

**Table 5: Top 10 strains by composite performance score**

| Strain | Host | Biofuel | Strategy | O2 | Mode | Titer (g/L) | Yield (g/g) | Prod (g/L/h) | Score |
|---|---|---|---|---|---|---|---|---|---|
| S0092 | Cupriavidus necator | Ethanol | Heterologous pathway | Anaerobic | Fed-batch | 6.46 | 0.497 | 0.144 | 41.1 |
| S0149 | Cupriavidus necator | Ethanol | Transport engineering | Anaerobic | Continuous | 5.9 | 0.51 | 0.05 | 40.6 |
| S0022 | Zymomonas mobilis | 2,3-Butanediol | CRISPRi tuning | Anaerobic | Batch | 3.97 | 0.5 | 0.056 | 38.5 |
| S0100 | Escherichia coli | Ethanol | Heterologous pathway | Aerobic | Batch | 7.19 | 0.449 | 0.066 | 37.5 |
| S0090 | Cupriavidus necator | Biojet (FAEE) | Promoter library tuning | Microaerobic | Fed-batch | 21.93 | 0.217 | 0.301 | 34.6 |
| S0014 | Cupriavidus necator | Isobutanol | Overexpression | Anaerobic | Batch | 6.07 | 0.41 | 0.086 | 34.1 |
| S0127 | Saccharomyces cerevisiae | Isobutanol | Knockout | Aerobic | Continuous | 4.84 | 0.41 | 0.074 | 33.1 |
| S0172 | Saccharomyces cerevisiae | Ethanol | Knockout | Anaerobic | Batch | 4.28 | 0.419 | 0.046 | 33 |
| S0001 | Saccharomyces cerevisiae | 2,3-Butanediol | CRISPRi tuning | Anaerobic | Batch | 3.6 | 0.427 | 0.032 | 32.9 |
| S0142 | Escherichia coli | Ethanol | Heterologous pathway | Microaerobic | Batch | 1.54 | 0.413 | 0.043 | 30.5 |

Table 6 reports Pearson correlation coefficients between key biochemical and process-level drivers and the three primary production outputs: titer, yield, and productivity. This table is central to the biochemical interpretation of the dataset, as it distinguishes *direct metabolic drivers* of performance from variables that are commonly assumed to be important but show limited explanatory power in practice. The strongest positive correlations with both titer and productivity are observed for acetyl-CoA flux and acetyl-CoA supply, confirming that precursor availability at the acetyl-CoA node is a dominant determinant of biofuel output across diverse hosts and products. This finding aligns with established metabolic theory, as acetyl-CoA functions as a key branching point for alcohols, fatty-acid-derived fuels, and isoprenoids. The weaker correlation between acetyl-CoA supply and yield further suggests that high precursor availability primarily enhances volumetric output rather than conversion efficiency. Product pathway activity also shows consistently positive correlations across all three outputs, particularly yield and productivity. This indicates that downstream pathway capacity not merely upstream carbon supply is essential for translating metabolic potential into measurable production gains. In contrast, glycolytic and pentose phosphate pathway activities display weak or inconsistent correlations, highlighting that upstream

carbon processing alone is insufficient without effective flux channeling toward the product sink. Notably, ATP turnover rate and redox ratios (NAD/NADH and NADP/NADPH) exhibit weak or slightly negative correlations with production metrics. This challenges the common assumption that increased cellular energy turnover directly supports higher production. Instead, the data suggest that elevated ATP demand and altered redox balance may reflect metabolic stress or maintenance costs rather than productive flux, reinforcing the concept of an energy–production trade-off. Finally, glucose uptake shows moderate correlation with productivity but weaker association with yield, indicating that increased substrate consumption accelerates production rate without necessarily improving efficiency. Overall, Table 6 demonstrates that biofuel performance is governed by *targeted flux control* at key metabolic nodes rather than global increases in metabolic activity. These correlations provide a mechanistic rationale for prioritizing acetyl-CoA-centric and pathway-capacity-focused engineering strategies in subsequent strain optimization efforts.

**Table 6: Pearson correlations: drivers vs outputs**

| Driver | Titer | Yield | Productivity |
|---|---|---|---|
| glycolysis activity rel | -0.021 | 0.124 | 0.018 |
| PPP activity rel | 0.105 | -0.121 | 0.098 |
| acetylCoA supply rel | 0.456 | 0.036 | 0.483 |
| redox engineering rel | 0.216 | 0.12 | 0.205 |
| product pathway activity rel | 0.423 | 0.408 | 0.404 |
| glucose uptake mmol gDW h | 0.274 | -0.027 | 0.297 |
| acetylCoA flux mmol gDW h | 0.581 | 0.044 | 0.651 |
| NADH generation mmol gDW h | 0.176 | 0.122 | 0.239 |
| NADPH generation mmol gDW h | 0.234 | -0.038 | 0.254 |
| ATP turnover rate mmol gDW h | -0.075 | 0.081 | -0.019 |
| NAD NADH ratio | -0.073 | -0.068 | -0.085 |
| NADP NADPH ratio | 0.01 | 0.045 | 0 |

Table 7 examines how oxygen regime (aerobic, anaerobic, and microaerobic) shapes intracellular redox balance, energy turnover, and growth rate across engineered strains. This table is physiologically important because oxygen availability directly constrains electron transport, cofactor recycling, and ATP generation, thereby influencing the feasibility and efficiency of biofuel production pathways. Aerobic conditions exhibit the highest mean ATP turnover rate and specific growth rate, reflecting efficient oxidative phosphorylation and robust biomass formation. However, this energetic advantage is accompanied by comparatively lower relevance for biofuel production in many cases, as high growth rates often divert carbon and reducing equivalents away from product synthesis toward cellular maintenance. The relatively stable NAD/NADH and NADP/NADPH ratios under aerobic conditions further suggest tighter redox regulation, which favors metabolic stability but may limit the accumulation of reduced biofuel products. In contrast, anaerobic conditions show reduced ATP turnover and growth rates but comparable redox ratios, indicating that cells maintain cofactor balance despite diminished energy yield. This highlights a fundamental trade-off: although anaerobic metabolism is energetically less efficient, it often promotes product formation by limiting carbon loss to respiration and forcing

reductant utilization through fermentative pathways. The lower ATP availability may therefore indirectly enhance biofuel yields by constraining biomass accumulation and redirecting flux toward product sinks. Microaerobic conditions occupy an intermediate physiological state, with ATP turnover and growth rates higher than anaerobic but lower than fully aerobic cultures. The slightly elevated variability in redox ratios under microaerobic conditions suggests sensitivity to fine-scale oxygen control, which can either stabilize production or induce metabolic stress depending on the strain and pathway. This explains why microaerobic regimes frequently appear among high-performing strains but rarely dominate uniformly. Overall, Table 7 demonstrates that oxygen regime acts as a *global metabolic regulator* rather than a simple on–off switch for production. Optimal biofuel performance emerges not from maximizing energy generation but from carefully balancing redox stability, ATP demand, and growth suppression. These findings reinforce the necessity of tailoring oxygen control to both host physiology and target product chemistry, rather than assuming aerobic conditions are inherently superior for engineered biofuel systems.

**Table 7: Redox and energy metrics by oxygen regime (mean and SD)**

| O2 regime | NAD/NADH_mean | NAD/NADH_SD | NADP/NADPH_mean | NADP/NADPH_SD | ATP_mean | ATP_SD | mu_mean | mu_SD |
|---|---|---|---|---|---|---|---|---|
| Aerobic | 2.043 | 0.522 | 2.648 | 0.628 | 18.812 | 8.996 | 0.305 | 0.119 |
| Anaerobic | 2.101 | 0.667 | 2.564 | 0.694 | 15.344 | 7.091 | 0.224 | 0.1 |
| Microaerobic | 2.181 | 0.793 | 2.65 | 0.681 | 15.239 | 7.262 | 0.239 | 0.09 |

Figure 1 presents a principal component analysis (PCA) integrating key biochemical drivers and production performance metrics to elucidate dominant sources of variability across engineered strains. The PCA reduces the high-dimensional dataset into two orthogonal components, enabling interpretation of underlying metabolic trade-offs that are not apparent from univariate comparisons alone . The first principal component (PC1) captures the largest proportion of variance and is strongly aligned with biofuel titer, productivity, and acetyl-CoA–related variables. This axis can be interpreted as a production-oriented carbon flux dimension, indicating that strains positioned toward the positive side of PC1 are characterized by enhanced precursor availability and efficient channeling of carbon toward the target product. The co-alignment of acetyl-CoA supply and acetyl-CoA flux with performance outputs reinforces the central role of this metabolic node as a bottleneck governing volumetric production across diverse hosts and biofuels. In contrast, the second principal component (PC2) is dominated by ATP turnover and redox-related variables, representing an energetic and redox constraint axis. Strains with higher PC2 scores exhibit elevated energy demand and altered cofactor balance, which does not consistently translate into improved production. This separation highlights a critical insight: increased metabolic activity and energy turnover are not inherently beneficial for biofuel synthesis and may instead reflect maintenance costs or stress responses that compete with product formation. The near-orthogonality between production-associated variables (PC1) and energy/redox variables (PC2) demonstrates a fundamental trade-off in metabolic engineering. Strains optimized for high biofuel output tend to prioritize carbon flux redirection over maximal energy efficiency, whereas energetically robust strains may sustain growth without achieving superior production metrics. Importantly, the dispersion of strains across both components indicates that no single metabolic state universally optimizes all objectives. Overall, Figure 1 provides a systems-level validation of the dataset structure and supports the subsequent correlation and strategy-level analyses. By explicitly separating carbon flux control from energetic constraints, the PCA confirms that successful biofuel engineering requires targeted manipulation of key metabolic nodes rather than global amplification of cellular metabolism.

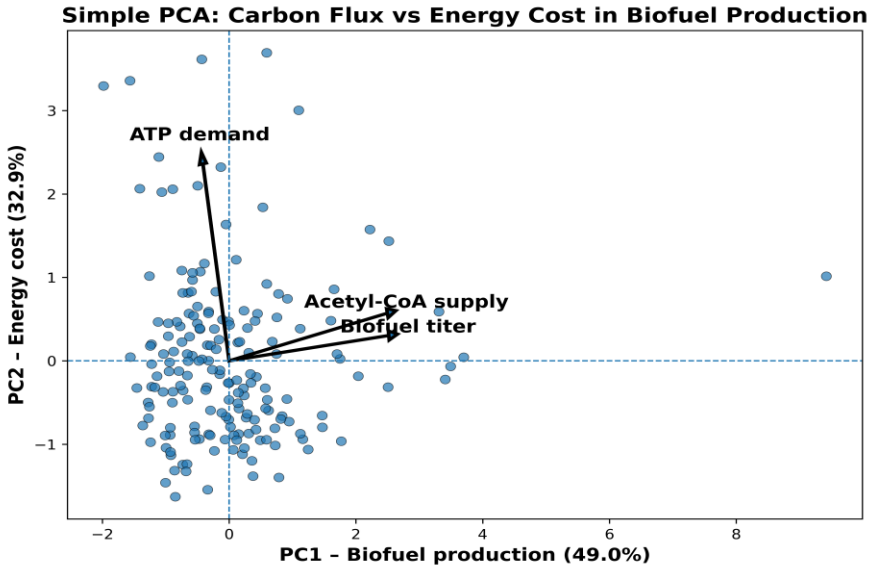


**Figure 1: Principal Component Analysis (PCA) of Biochemical Drivers and Biofuel Production Performance**

Figure 2 presents a normalized radar plot comparing the relative pathway capacities of the top-performing metabolic engineering strategies. By visualizing multiple pathway-level indicators simultaneously, this figure highlights how different strategies redistribute metabolic capacity rather than uniformly enhancing all pathways. Each axis in the radar plot represents a core metabolic function glycolysis, pentose phosphate pathway (PPP), acetyl-CoA supply, redox balancing capacity, and product pathway activity normalized to enable direct comparison across strategies. The use of normalization is critical, as it emphasizes relative prioritization of pathways rather than absolute magnitude, allowing interpretation of engineering intent and metabolic trade-offs. Strategies exhibiting broad, evenly expanded radar profiles indicate holistic metabolic reprogramming. For example, approaches such as transport engineering and cofactor engineering show relatively balanced enhancement across precursor supply, redox handling, and product pathway capacity. This suggests that these strategies improve system-level efficiency by alleviating bottlenecks and coordinating flux distribution, which may explain their moderate but consistent performance observed in Table 4. In contrast, strategies with pronounced spikes along specific axes such as promoter library tuning or heterologous pathway introduction—reflect targeted amplification of selected pathways. While these focused interventions can generate high peak performance, their narrower profiles indicate potential vulnerabilities, such as redox imbalance or precursor limitation, that may reduce robustness across conditions. This visual pattern aligns with the high variability associated with these strategies in downstream performance metrics. Notably, enhancement of glycolysis and PPP alone does not guarantee expansion of acetyl-CoA or product pathway capacity, reinforcing the conclusion that upstream carbon processing must be coupled with downstream flux sinks to yield productive outcomes. Similarly, redox capacity emerges as a supporting rather than dominant dimension, enabling pathway function but rarely acting as the primary driver of performance. Overall, Figure 2 demonstrates that successful metabolic engineering is characterized by strategic reallocation of metabolic capacity rather than indiscriminate pathway upregulation. The radar plot provides an intuitive yet mechanistically grounded comparison of engineering

philosophies, reinforcing the idea that balanced pathway coordination is often more effective and reliable than aggressive, single-pathway optimization.

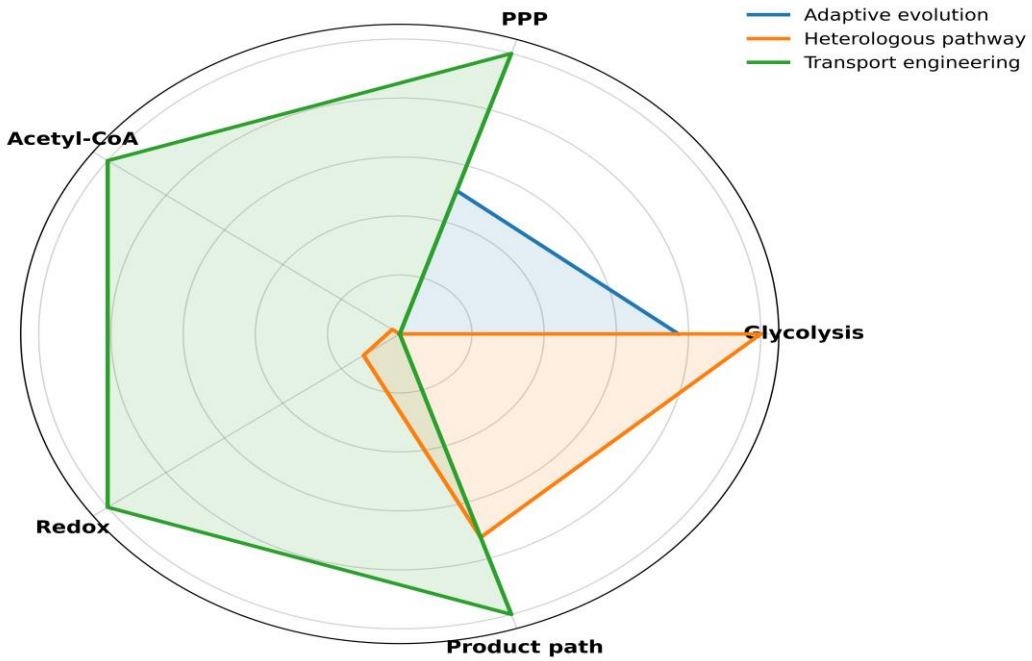


**Figure 2: Normalized Pathway-Capacity Radar Comparison of Engineering Strategies**

Figure 3 presents a correlation heatmap illustrating the strength and direction of relationships between key biochemical drivers and biofuel production outputs (titer, yield, and productivity). Unlike univariate comparisons, this figure enables rapid identification of dominant metabolic determinants while simultaneously highlighting variables with limited explanatory power. The heatmap reveals that acetyl-CoA–related variables, particularly acetyl-CoA flux, exhibit the strongest positive correlations with both titer and productivity. This confirms that effective routing of carbon through the acetyl-CoA node is a central requirement for achieving high volumetric output, irrespective of host organism or target biofuel. Product pathway activity also shows consistently positive correlations across all output metrics, emphasizing that downstream pathway capacity is essential for converting precursor availability into realized production gains. In contrast, glycolytic and pentose phosphate pathway activities display weak or inconsistent correlations with performance. This finding is mechanistically important, as it demonstrates that increasing upstream carbon processing alone does not guarantee improved biofuel synthesis. Without sufficient downstream capacity or precursor channeling, enhanced glycolysis may primarily support growth or maintenance rather than product formation. Similarly, moderate correlations between glucose uptake and productivity but not yield suggest that higher substrate consumption accelerates production rate at the expense of efficiency. Redox-related variables and ATP turnover rate show weak or slightly negative correlations with production outputs. This challenges the common assumption that increased energy generation or redox cycling directly supports higher biofuel yields. Instead, these variables likely reflect metabolic burden or stress responses, where energy and reducing equivalents are diverted toward cellular survival rather than productive synthesis. The near-zero correlations of NAD/NADH and NADP/NADPH ratios further suggest that maintaining redox balance is a prerequisite for viability but not a strong driver of enhanced

output. Overall, Figure 3 reinforces a key principle of metabolic engineering: biofuel performance is governed by targeted control of flux at critical metabolic nodes, not by global amplification of metabolic activity. The correlation structure provides a mechanistic rationale for prioritizing acetyl-CoA-centric and pathway-capacity-focused strategies, while cautioning against overinvestment in broadly increasing upstream metabolism without coordinated downstream optimization.

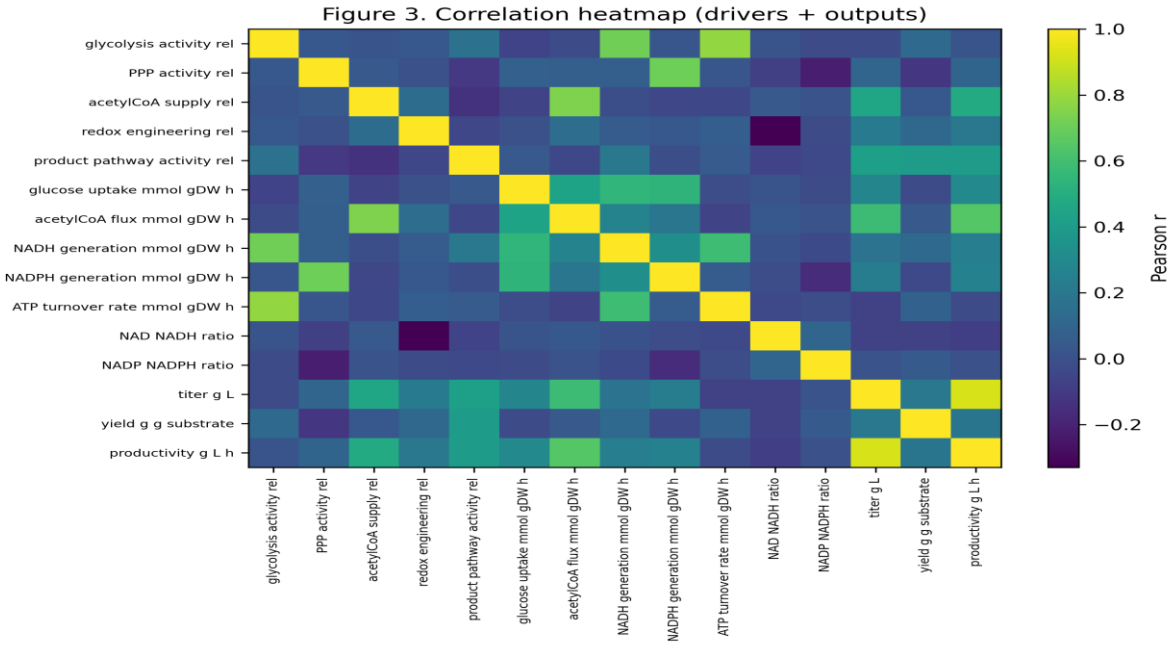


**Figure 3: Correlation Heatmap of Biochemical Drivers and Production Outputs**

Figure 4 presents a boxplot comparison of final biofuel titers across different target biofuels, enabling assessment of both central tendency and variability in production outcomes. Unlike mean-based summaries, the boxplot format highlights dispersion, skewness, and the presence of high-performing outliers, which are particularly relevant in metabolic engineering datasets characterized by heterogeneous strain performance. The figure shows that ethanol and fatty-acid-derived biofuels (such as biodiesel and biojet fuels) generally achieve higher median titers compared to other products. However, these biofuels also exhibit wider interquartile ranges and more pronounced outliers, indicating substantial variability among engineered strains. This suggests that while high titers are achievable for these products, success is highly dependent on precise alignment between host metabolism, pathway engineering, and cultivation conditions. High median performance therefore reflects *potential* rather than guaranteed outcomes. In contrast, biofuels such as isobutanol, isoprene, and 2,3-butanediol display lower median titers with comparatively narrower distributions. This reduced variability implies stronger intrinsic biochemical constraints, such as limited precursor availability, redox imbalance, or product toxicity, which restrict maximum achievable concentrations regardless of engineering effort. While these products may be more challenging to scale in terms of concentration, their tighter distributions suggest greater predictability across strains. Importantly, the presence of outliers above the upper quartile for several biofuels demonstrates that exceptional performance is possible even within constrained product classes. These outliers likely represent optimized combinations of host selection and targeted pathway engineering, reinforcing the

value of strain-specific optimization rather than broad strategy generalization. Overall, Figure 4 illustrates that biofuel titer is not uniformly distributed across product classes and cannot be reliably inferred from average values alone. The figure underscores the importance of considering variability and robustness when evaluating production feasibility. High median titers indicate promising biofuel targets, but wide dispersion signals increased developmental risk, whereas narrower distributions suggest more stable yet potentially limited production ceilings. This distributional perspective complements earlier multivariate and correlation analyses by contextualizing production outcomes within realistic biological variability.

Figure 4. Distribution of titer by target biofuel

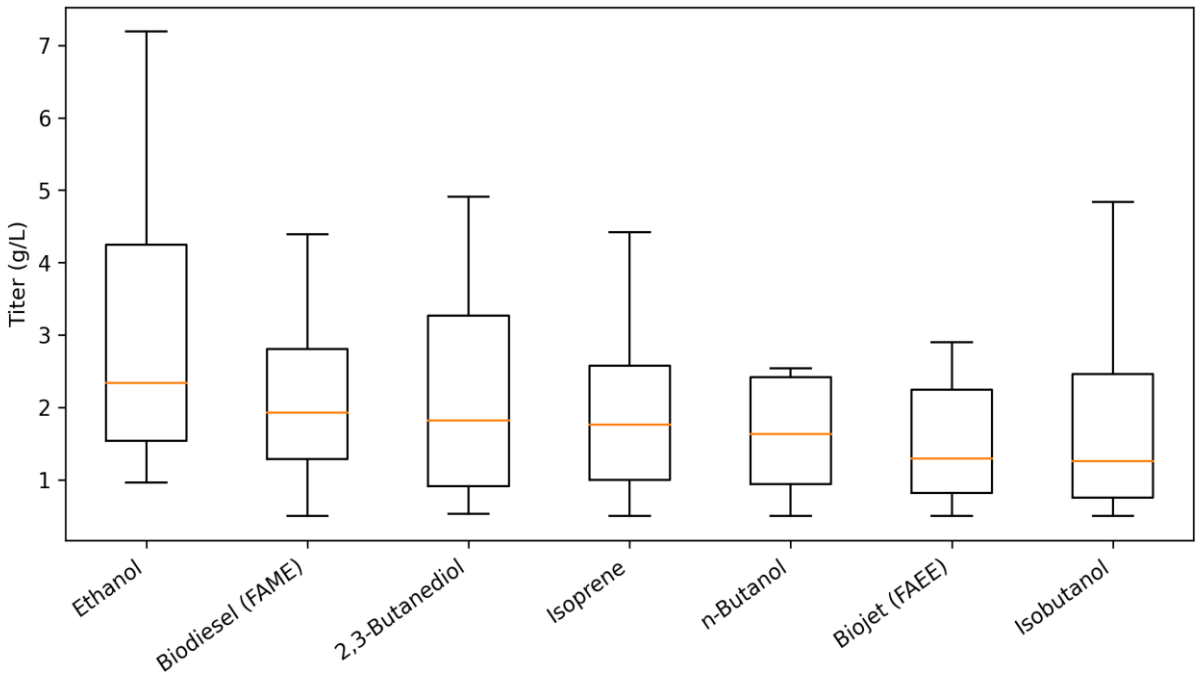


**Figure 4: Distribution of Biofuel Titer across Different Target Biofuels**

Figure 5 presents a bubble scatter plot illustrating the relationship between final biofuel titer and volumetric productivity, with bubble size representing yield. This three-dimensional visualization is particularly effective for highlighting multi-objective trade-offs that cannot be captured through pairwise comparisons alone. By simultaneously representing concentration, production rate, and substrate efficiency, the figure provides an integrated view of biofuel production performance. The distribution of data points shows a clear positive association between titer and productivity for a subset of strains, indicating that improvements in concentration can, under optimized conditions, coincide with faster production rates. However, this trend is not universal. A substantial proportion of strains achieve moderate productivity at relatively low titers, suggesting that increased production rate may result from rapid substrate consumption rather than sustained product accumulation. This distinction is critical for industrial relevance, as short-term productivity gains may not translate into economically viable final concentrations. Bubble size variation further reveals that high yield does not consistently align with either high titer or high productivity. Several large bubbles appear at intermediate productivity and titer values, indicating strains that efficiently convert substrate into product but do not reach extreme concentrations or rates. Conversely, some high-

titer and high-productivity strains exhibit smaller bubble sizes, reflecting reduced conversion efficiency due to increased maintenance energy, by-product formation, or metabolic burden. This visual decoupling reinforces the concept that yield, titer, and productivity are governed by partially independent metabolic constraints. The log-scaled titer axis highlights clustering at low concentrations, emphasizing that high-titer strains are relatively rare and represent optimized outliers rather than typical outcomes. These high-performing strains occupy the upper-right region of the plot, illustrating the difficulty of simultaneously maximizing all three performance metrics. Overall, Figure 5 demonstrates that biofuel production optimization is inherently multi-dimensional. Maximizing one metric often compromises another, and superior strains must be evaluated based on balanced performance rather than extreme values in a single dimension. The figure provides strong visual evidence supporting the use of composite performance metrics and multi-objective optimization strategies in metabolic engineering research.

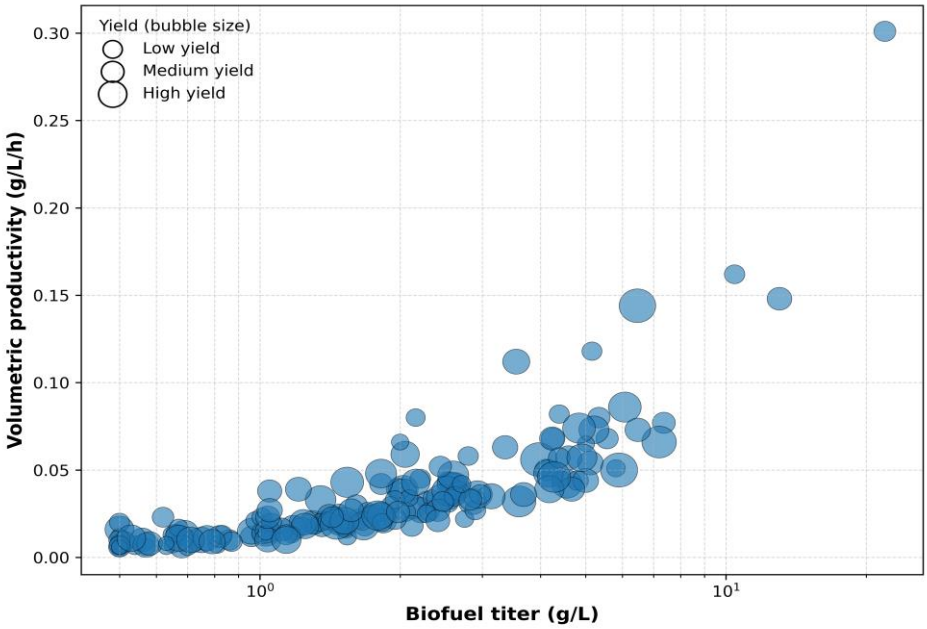


**Figure 5: Relationship between Biofuel Titer and Volumetric Productivity with Yield as a Third Dimension**

Figure 6 presents a bar-based comparison of the top-ranked engineered strains, highlighting their relative performance across the three core biofuel production metrics: titer, yield, and volumetric productivity. By focusing exclusively on the highest-scoring strains, this figure shifts the analysis from population-level trends to elite performance profiles, enabling clearer identification of practical trade-offs relevant for strain selection and scale-up. The normalized bar representation allows direct comparison across metrics with different units and magnitudes, ensuring that no single metric visually dominates the interpretation. The figure clearly shows that none of the top strains simultaneously maximizes all three performance dimensions. Some strains achieve superior titer but display comparatively lower yield or productivity, indicating effective product accumulation at the cost of substrate efficiency or production rate. Conversely, strains with high yield often exhibit moderate titer and productivity, suggesting that efficient carbon conversion does not necessarily result in rapid or high-level product accumulation. Productivity

patterns further emphasize this trade-off structure. Strains with elevated productivity frequently sacrifice yield, implying accelerated substrate uptake and metabolic throughput that may increase maintenance energy demands or by-product formation. This observation aligns with the correlation trends identified in Figure 3 and reinforces the notion that high production rates are not inherently synonymous with metabolic efficiency. Importantly, the figure demonstrates that performance ranking is sensitive to the weighting of metrics. A strain appearing dominant in one dimension may be less attractive when evaluated under multi-objective criteria. This highlights the limitation of selecting strains based solely on single metrics such as titer and supports the use of composite performance scores or application-specific prioritization frameworks. Overall, Figure 6 underscores that top-performing biofuel strains are defined not by absolute superiority but by *balanced optimization*. The figure provides a practical decision-making tool, allowing researchers to match strain performance profiles with specific industrial objectives, such as maximizing throughput, minimizing feedstock consumption, or achieving stable intermediate performance. In doing so, it reinforces the central conclusion of this study: successful metabolic engineering requires strategic compromise rather than unidimensional optimization.

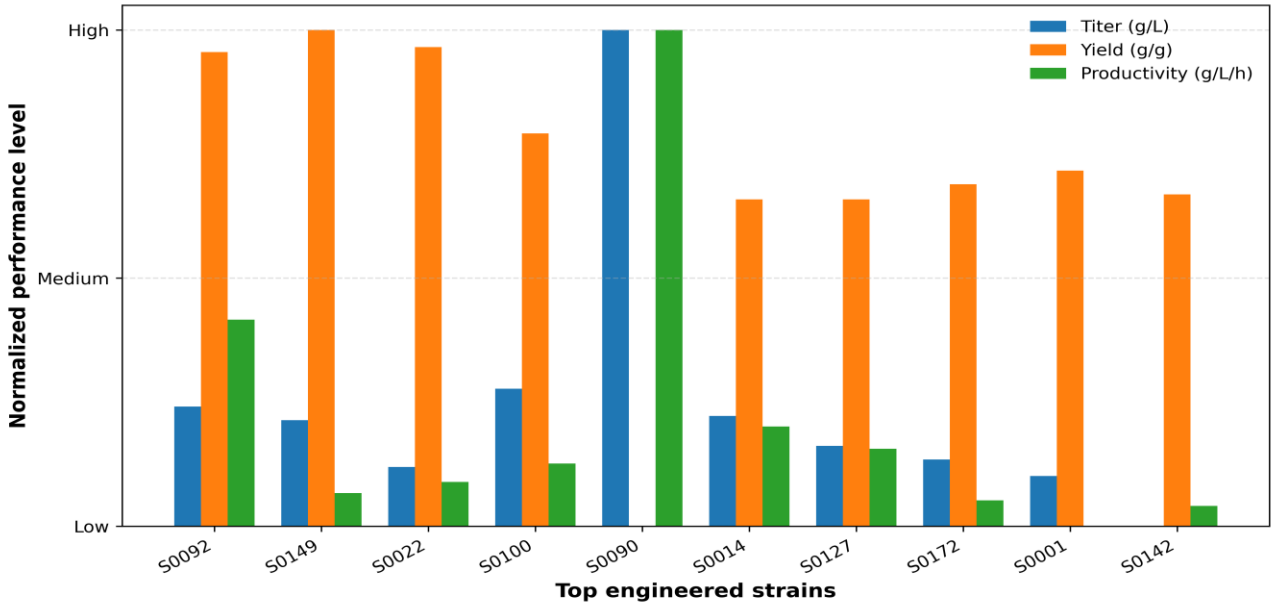


**Figure 6: Comparative Performance of Top-Ranked Engineered Strains across Key Metrics**

## Conclusion

This study examined the biochemical determinants of enhanced biofuel production in metabolically engineered microorganisms through an integrated, systems-level analytical framework. By jointly analysing pathway capacity indicators, intracellular flux proxies, redox balance, energy turnover, and production outputs, the work moves beyond single-metric or pathway-isolated interpretations that dominate much of the existing literature. The results consistently demonstrate that biofuel performance is governed by targeted control of carbon flux at key metabolic nodes rather than by indiscriminate amplification of global metabolic activity. Across all analyses, acetyl-CoA availability emerged as the dominant driver of biofuel titer and productivity, confirming its role as a central

bottleneck in microbial biofuel synthesis. However, the study also shows that enhanced precursor supply alone is insufficient to guarantee efficient production. Without adequate downstream pathway capacity, carbon redirection leads to metabolic congestion and by-product formation rather than improved yield. This finding reinforces the necessity of coordinated pathway engineering, where upstream flux enhancement is matched with proportional expansion of product sinks. Redox balance and energy metabolism were shown to function primarily as constraints rather than direct drivers of production. Elevated ATP turnover and altered NAD(H)/NADP(H) ratios did not correlate positively with improved performance, indicating that energetic robustness and high growth rates often compete with product-oriented metabolism. Oxygen regime further modulated these effects, with anaerobic and microaerobic conditions frequently favoring production by suppressing respiratory carbon loss, despite lower energetic efficiency. These observations challenge the common assumption that maximizing cellular energy generation inherently benefits biofuel synthesis. Importantly, no single engineering strategy or strain configuration universally optimized titer, yield, and productivity simultaneously. High-performing strains achieved success through balanced trade-offs rather than absolute dominance in any one metric. This underscores the inadequacy of unidimensional optimization approaches and supports the adoption of multi-objective evaluation frameworks in strain selection and process design. While the study is based on a synthetic, biochemically constrained dataset rather than direct experimentation, its value lies in clarifying system-level relationships that are difficult to isolate experimentally. The findings provide a mechanistic rationale for prioritizing acetyl-CoA–centric, pathway-capacity-aligned engineering strategies while explicitly accounting for energetic and redox limitations. Future experimental work should build on these insights to validate context-specific interventions, rather than pursuing universal optimization paradigms.

**References**

Stephanopoulos, G. (2012). Metabolic engineering: perspectives of a discipline in flux. *Metabolic Engineering*, 14(3), 189–190.

Nielsen, J., & Keasling, J. D. (2016). Engineering cellular metabolism. *Cell*, 164(6), 1185–1197.

Keasling, J. D. (2010). Manufacturing molecules through metabolic engineering. *Science*, 330(6009), 1355–1358.

Lee, S. Y., Kim, H. U., & Park, J. H. (2012). Metabolic engineering of microorganisms for biofuels production. *Current Opinion in Biotechnology*, 23(3), 392–399.

Chubukov, V., Mukhopadhyay, A., Petzold, C. J., Keasling, J. D., & Martín, H. G. (2016). Synthetic and systems biology for microbial production of commodity chemicals. *NPJ Systems Biology and Applications*, 2, 16009.

Clomburg, J. M., & Gonzalez, R. (2010). Biofuel production in *Escherichia coli*: the role of metabolic engineering and synthetic biology. *Applied Microbiology and Biotechnology*, 86(2), 419–434.

Atsumi, S., Hanai, T., & Liao, J. C. (2008). Non-fermentative pathways for synthesis of branched-chain higher alcohols as biofuels. *Nature*, 451(7174), 86–89.

Peralta-Yahya, P. P., Zhang, F., del Cardayre, S. B., & Keasling, J. D. (2012). Microbial engineering for the production of advanced biofuels. *Nature*, 488(7411), 320–328.

Lee, J. W., Na, D., Park, J. M., Lee, J., Choi, S., & Lee, S. Y. (2012). Systems metabolic engineering of microorganisms for natural and non-natural chemicals. *Nature Chemical Biology*, 8(6), 536–546.

Zhao, X., Nielsen, J., & Olafsson, S. (2020). Systems biology approaches to metabolic engineering. *Current Opinion in Biotechnology*, 64, 142–149.

Kim, J. H., Block, D. E., & Mills, D. A. (2010). Simultaneous consumption of pentose and hexose sugars: an optimal microbial phenotype for efficient fermentation of lignocellulosic biomass. *Applied Microbiology and Biotechnology*, 88(5), 1077–1085.

Qian, Z. G., Xia, X. X., & Lee, S. Y. (2011). Metabolic engineering of *Escherichia coli* for the production of putrescine. *Metabolic Engineering*, 13(3), 278–287.

Wehrs, M., Tanjore, D., Eng, T., Lievense, J., Pray, T. R., & Mukhopadhyay, A. (2019). Engineering robust production microbes for large-scale cultivation. *Trends in Microbiology*, 27(6), 524–537.

Khan, R., Khan, A., Muhammad, I., & Khan, F. (2025). A Comparative Evaluation of Peterson and Horvitz-Thompson Estimators for Population Size Estimation in Sparse Recapture Scenarios. *Journal of Asian Development Studies*, *14*(2), 1518-1527.

Bommareddy, R. R., Chen, Z., Rappert, S., & Zeng, A. P. (2014). A de novo NADH regeneration system for improving anaerobic growth and succinate production in *Escherichia coli*. *Metabolic Engineering*, 26, 1–10.

Liu, L., Redden, H., & Alper, H. S. (2013). Frontiers of yeast metabolic engineering: diversifying beyond ethanol and Saccharomyces. *Current Opinion in Biotechnology*, 24(6), 1023–1030.

KHAN, R., SHAH, A. M., & KHAN, H. U. (2025). Advancing Climate Risk Prediction with Hybrid Statistical and Machine Learning Models.

Zhu, Z., Zhang, S., Liu, H., Shen, H., Lin, X., Yang, F., Zhou, Y., Jin, G., Ye, M., Zou, H., & Zhao, Z. K. (2017). A multi-omic map of the lipid-producing yeast *Yarrowia lipolytica*. *Nature Communications*, 8, 1486.

Sumeer, A., Ullah, F., Khan, S., Khan, R., & Khan, W. (2025). Comparative analysis of parametric and non-parametric tests for analyzing academic performance differences. *Policy Research Journal*, *3*(8), 55-62.

Kildegaard, K. R., Jensen, N. B., Schneider, K., Czarnotta, E., Özdemir, E., Klein, T., & Nielsen, J. (2016). Engineering of *Saccharomyces cerevisiae* for the production of the advanced biofuel isobutanol. *Metabolic Engineering*, 34, 1–10.

Varman, A. M., He, L., Follenfant, R., Wu, W., Wemmer, S., Wrobel, S. A., Tang, Y. J., & Singh, S. (2013). Hybrid phenotypes for robust biofuel production. *Nature Communications*, 4, 2031.

Bhatia, S. K., Kim, S. H., Yoon, J. J., & Yang, Y. H. (2017). Current status and strategies for second generation biofuel production using microbial systems. *Energy Conversion and Management*, 148, 1142–1156.

Nielsen, J. (2017). Systems biology of metabolism: a driver for developing personalized and precision medicine. *Cell Metabolism*, 25(3), 572–579.

Khan, R., Shah, A. M., Ijaz, A., & Sumeer, A. (2025). Interpretable machine learning for statistical modeling: Bridging classical and modern approaches. *International Journal of Social Sciences Bulletin*, *3*(8), 43-50.

Sauer, U. (2007). Metabolic networks in motion: 13C-based flux analysis. *Molecular Systems Biology*, 3, 129.

Orth, J. D., Thiele, I., & Palsson, B. Ø. (2010). What is flux balance analysis? *Nature Biotechnology*, 28(3), 245–248.

Kim, H. U., Kim, T. Y., & Lee, S. Y. (2008). Metabolic flux analysis and metabolic engineering of microorganisms. *Molecular BioSystems*, 4(2), 113–120.

Zhang, F., Carothers, J. M., & Keasling, J. D. (2012). Design of a dynamic sensor-regulator system for production of chemicals and fuels derived from fatty acids. *Nature Biotechnology*, 30(4), 354–359.

Van Dien, S. (2013). From the first drop to the first truckload: commercialization of microbial processes for renewable chemicals. *Current Opinion in Biotechnology*, 24(6), 1061–1068.